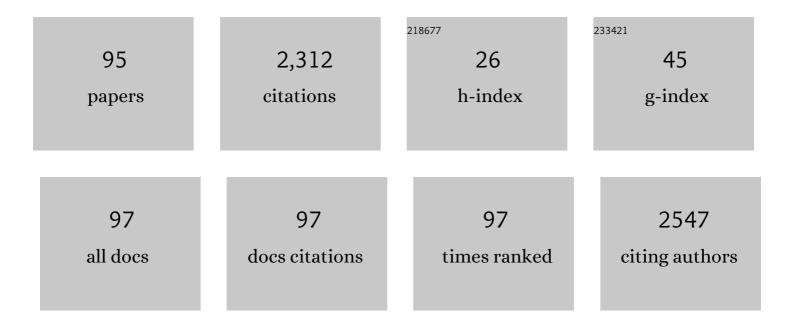
List of Publications by Year in descending order

Source: https://exaly.com/author-pdf/5623013/publications.pdf Version: 2024-02-01



#	Article	IF	CITATIONS
1	Uniform Organically Modified CeO ₂ Nanoparticles Synthesized from a Carboxylate Complex under Supercritical Hydrothermal Conditions: Impact of Ce Valence. Journal of Physical Chemistry C, 2022, 126, 6008-6015.	3.1	4
2	The difference of PMMAâ€brushâ€modification on the oxygen permeable perovskiteâ€type oxides by consisting elements. Journal of the American Ceramic Society, 2021, 104, 4932-4937.	3.8	2
3	Quantitative evaluation of the intratumoral distribution of platinum in oxaliplatinâ€treated rectal cancer: <i>In situ</i> visualization of platinum <i>via</i> synchrotron radiation Xâ€ray fluorescence spectrometry. International Journal of Cancer, 2020, 146, 2498-2509.	5.1	6
4	Analysis of the dynamic behavior and local structure of solid-solution carbon in age-hardened low-carbon steels by soft X-ray absorption spectroscopy. Materialia, 2020, 14, 100876.	2.7	5
5	Observation of Chemical State for Interstitial Solid Solution of Carbon in Low-carbon Steel by Soft X-ray Absorption Spectroscopy. ISIJ International, 2020, 60, 114-119.	1.4	1
6	Control of crystal structure and performance evaluation of multi-piezo material of Li _{1â^'} <i>_x</i> Na <i>_xJournal of the Ceramic Society of Japan, 2020, 128, 518-522.</i>	g t,N bO&l	t;sub>3&l
7	PM oxidation over Ag-loaded perovskite-type oxide catalyst prepared by thermal decomposition of heteronuclear cyano-complex precursor. Catalysis Today, 2019, 332, 83-88.	4.4	3
8	Oxygen sorption-desorption properties and order–disorder transitions on La–Sr–Co–Fe perovskite-type oxides. Journal of the Ceramic Society of Japan, 2019, 127, 378-382.	1.1	1
9	Thermoelectric gas sensors with selective combustion catalysts. Journal of the Ceramic Society of Japan, 2019, 127, 57-66.	1.1	7
10	Preparation of High-Density Polymer Brushes with a Multihelical Structure. Langmuir, 2018, 34, 3283-3288.	3.5	10
11	Selective Oxidation of Thioanisole with Hydrogen Peroxide using Copper Complexes Encapsulated in Zeolite: Formation of a Thermally Stable and Reactive Copper Hydroperoxo Species. ACS Catalysis, 2018, 8, 2645-2650.	11.2	28
12	Observation of Chemical State for Interstitial Solid Solution of Carbon in Low-carbon Steel by Soft X-ray Absorption Spectroscopy. Tetsu-To-Hagane/Journal of the Iron and Steel Institute of Japan, 2018, 104, 628-633.	0.4	3
13	Depth-Resolved Characterization of Perylenediimide Side-Chain Polymer Thin Film Structure Using Grazing-Incidence Wide-Angle X-ray Diffraction with Tender X-rays. Langmuir, 2018, 34, 8516-8521.	3.5	9
14	Ground-State Copper(III) Stabilized by N-Confused/N-Linked Corroles: Synthesis, Characterization, and Redox Reactivity. Journal of the American Chemical Society, 2018, 140, 6883-6892.	13.7	45
15	Determination of Effective Oxygen Adsorption Species for CO Sensing Based on Electric Properties of Indium Oxide. Journal of the Electrochemical Society, 2018, 165, B275-B280.	2.9	19
16	Morphology, microstructure, and surface area of La-added MgFe ₂ O ₄ powder. Journal of the Ceramic Society of Japan, 2018, 126, 402-407.	1.1	7
17	Solvent-free, improved synthesis of pure bixbyite phase of iron and manganese mixed oxides as low-cost, potential oxygen carrier for chemical looping with oxygen uncoupling. Pure and Applied Chemistry, 2017, 89, 511-521.	1.9	9
18	Soot oxidation performance with a HZSM-5 supported Ag nanoparticles catalyst and the characterization of Ag species. RSC Advances, 2017, 7, 43789-43797.	3.6	9

#	Article	IF	CITATIONS
19	Bisâ€Copper(II)/Ï€â€Radical Multiâ€Heterospin System with Nonâ€innocent Doubly <i>N</i> â€Confused Dioxohexaphyrin(1.1.1.1.10) Ligand. Chemistry - A European Journal, 2017, 23, 15322-15326.	3.3	16
20	Effect of Thermal Conductivity of Catalytic Materials on Soot Sensing Performance Based on a Combustion-type Sensor. Chemistry Letters, 2017, 46, 1304-1307.	1.3	0
21	Soot Oxidation Activity of Ag/HZSM-5 (Si/Al=40) Catalyst. Evergreen, 2017, 4, 7-11.	0.5	1
22	Solvent free oxidative coupling polymerization of 3-hexylthiophene (3HT) in the presence of FeCl ₃ particles. RSC Advances, 2016, 6, 111993-111996.	3.6	15
23	High Performance of SnO2-Based Gas Sensor by Introducing Perovskite-Type Oxides. ECS Transactions, 2016, 75, 31-37.	0.5	3
24	Micronization of MgFe ₂ O ₄ particles doped with Si. Journal of the Ceramic Society of Japan, 2016, 124, 777-780.	1.1	2
25	Xâ€ray absorption fine structure study on the role of solvent on polymerization of 3â€hexylthiophene with solid FeCl ₃ particles. Journal of Polymer Science Part A, 2015, 53, 2075-2078.	2.3	11
26	Temperature-programmed Desorption of Oxygen from La–Sr–Co–Fe Perovskite in Atmospheres with Varying Oxygen Partial Pressure. Chemistry Letters, 2015, 44, 357-359.	1.3	3
27	Formation of Tetravalent Fe Ions in LaFeO ₃ Perovskite Through Mechanochemical Modification by Ball Milling. Journal of the American Ceramic Society, 2015, 98, 1047-1051.	3.8	8
28	Improved catalytic activity of PrMO ₃ (M = Co and Fe) perovskites: synthesis of thermally stable nanoparticles by a novel hydrothermal method. New Journal of Chemistry, 2015, 39, 2342-2348.	2.8	22
29	Preparation and characterization of Pd loaded Sr-deficient K2NiF4-type (La, Sr)2MnO4 catalysts for NO–CO reaction. Catalysis Today, 2015, 251, 7-13.	4.4	7
30	Effects of Surface and Bulk Silver on PrMnO _{3+δ} Perovskite for CO and Soot Oxidation: Experimental Evidence for the Chemical State of Silver. ACS Catalysis, 2015, 5, 301-309.	11.2	55
31	Selective hydroxylation of cyclohexene over Fe-bipyridine complexes encapsulated into Y-type zeolite under environment-friendly conditions. Catalysis Today, 2015, 242, 261-267.	4.4	19
32	Ppm level methane detection using micro-thermoelectric gas sensors with Pd/Al2O3 combustion catalyst films. Sensors and Actuators B: Chemical, 2015, 206, 488-494.	7.8	49
33	Development of highly sensitive mechanoluminescent sensor aiming at small strain measurement. Journal of Advanced Dielectrics, 2014, 04, 1450016.	2.4	16
34	Copper–manganese mixed oxides: CO ₂ -selectivity, stable, and cyclic performance for chemical looping combustion of methane. Physical Chemistry Chemical Physics, 2014, 16, 19634-19642.	2.8	31
35	CO oxidation performance of Au/Co3O4 catalyst on the micro gas sensor device. Catalysis Today, 2013, 201, 85-91.	4.4	22
36	Thermoelectric gas sensor with CO combustion catalyst for ppm level carbon monoxide detection. Sensors and Actuators B: Chemical, 2013, 182, 789-794.	7.8	19

#	Article	IF	CITATIONS
37	Effects of noble metal addition on response of ceria thick film CO sensors. Sensors and Actuators B: Chemical, 2012, 171-172, 350-353.	7.8	33
38	Calibration Gas Preparation for Non-Disposable Portable MOx, PID, and IER VOC Detectors. Sensor Letters, 2012, 10, 985-992.	0.4	6
39	Thermoelectric hydrogen gas sensor. Synthesiology, 2011, 4, 99-107.	0.2	4
40	Thermoelectric gas sensors of different catalyst oxides and heater metals. IOP Conference Series: Materials Science and Engineering, 2011, 18, 212010.	0.6	1
41	Formation mechanism of monodispersed spherical core–shell ceria/polymer hybrid nanoparticles. Materials Research Bulletin, 2011, 46, 1168-1176.	5.2	39
42	Planar-type thermoelectric micro devices using ceramic catalytic combustor. Current Applied Physics, 2011, 11, S36-S40.	2.4	16
43	Microgenerator Using BiSbTe-Pt Thermopile and Pt-Al2O3 Ceramic Combustor. Journal of Electronic Materials, 2011, 40, 817-822.	2.2	6
44	Surface Organic Modification of In ₂ O ₃ Nanoparticle Assemblies and Their Flammable Gas Sensing Properties. Science of Advanced Materials, 2011, 3, 853-858.	0.7	1
45	Monitoring Breath Hydrogen Using Thermoelectric Sensor. Sensor Letters, 2011, 9, 684-687.	0.4	15
46	Alternating Current Impedance Analysis of CeO ₂ Thick Films as Odor Sensors. Sensor Letters, 2011, 9, 703-705.	0.4	5
47	Thermoelectric Micro-Multi-Gas Sensor for the Detection of Hydrogen, Carbon Monoxide and Methane. Sensor Letters, 2011, 9, 773-777.	0.4	2
48	Thermoelectric hydrogen sensors using Si and SiGe thin films with a catalytic combustor. Journal of the Ceramic Society of Japan, 2010, 118, 188-192.	1.1	17
49	XPS study of organic/MoO3 hybrid thin films for aldehyde gas sensors: correlation between average Mo valence and sensitivity. Journal of the Ceramic Society of Japan, 2010, 118, 171-174.	1.1	8
50	Pt catalytic effects on a resistive oxygen sensor using Ce0.9Zr0.1O2 thick film in rich conditions. Journal of the Ceramic Society of Japan, 2010, 118, 175-179.	1.1	1
51	Effects of High-Humidity Aging on Platinum, Palladium, and Gold Loaded Tin Oxide—Volatile Organic Compound Sensors. Sensors, 2010, 10, 6513-6521.	3.8	42
52	Microheater Meander Configurations for Combustion Catalysts in Thermoelectric Gas Sensor. Sensor Letters, 2010, 8, 792-800.	0.4	2
53	Resistive Oxygen Sensor Using Ceria-Zirconia Sensor Material and Ceria-Yttria Temperature Compensating Material for Lean-Burn Engine. Sensors, 2009, 9, 8884-8895.	3.8	26
54	Sensing performance of thermoelectric hydrogen sensor for breath hydrogen analysisâ~†. Sensors and Actuators B: Chemical, 2009, 137, 524-528.	7.8	43

4

#	Article	IF	CITATIONS
55	Fabrication of thermoelectric gas sensors on micro-hotplates. Sensors and Actuators B: Chemical, 2009, 139, 340-345.	7.8	25
56	Robust hydrogen detection system with a thermoelectric hydrogen sensor for hydrogen station application. International Journal of Hydrogen Energy, 2009, 34, 2834-2841.	7.1	48
57	Gas response, response time and selectivity of a resistive CO sensor based on two connected CeO2 thick films with various particle sizes. Sensors and Actuators B: Chemical, 2009, 136, 364-370.	7.8	52
58	High-Temperature Thermoelectric Measurement of B-Doped SiGe and Si Thin Films. Materials Transactions, 2009, 50, 1596-1602.	1.2	16
59	Ceramic catalyst combustors of Pt-loaded-alumina on microdevices. Journal of the Ceramic Society of Japan, 2009, 117, 659-665.	1.1	7
60	Preparation of core-shell type cerium oxide/polymer hybrid nanoparticles for ink-jet printing. Journal of the Ceramic Society of Japan, 2009, 117, 769-772.	1.1	13
61	Physicochemical properties and microstructures of core-shell type cerium oxide/organic polymer nanospheres. Journal of the Ceramic Society of Japan, 2009, 117, 773-776.	1.1	13
62	Preparation of layered organic–inorganic nanohybrid thin films of molybdenum trioxide with polyaniline derivatives for aldehyde gases sensors of several tens ppb level. Sensors and Actuators B: Chemical, 2008, 128, 512-520.	7.8	60
63	Fabrication and performance of free-standing hydrogen gas sensors. Sensors and Actuators B: Chemical, 2008, 129, 1-9.	7.8	14
64	Thermopile sensor-devices for the catalytic detection of hydrogen gas. Sensors and Actuators B: Chemical, 2008, 130, 200-206.	7.8	23
65	Long-term stability of Pt/alumina catalyst combustors for micro-gas sensor application. Journal of the European Ceramic Society, 2008, 28, 2183-2190.	5.7	25
66	Electrode contact study for SiGe thin film operated at high temperature. Applied Surface Science, 2008, 254, 4999-5006.	6.1	2
67	Characterizations of interlayer organic–inorganic nanohybrid of molybdenum trioxide with polyaniline and poly(o-anisidine). Materials Chemistry and Physics, 2008, 110, 115-119.	4.0	8
68	VOCs sensing properties of layered organic–inorganic hybrid thin films: MoO3 with various interlayer organic components. Materials Letters, 2008, 62, 3021-3023.	2.6	26
69	Resistive Type Sensor Using Ceria Thick Film with Nano Particles. Advanced Materials Research, 2008, 47-50, 1522-1525.	0.3	1
70	13C CP/MAS NMR Study of Cross-linked Poly(vinylpyrrolidone) on Surface of Cerium Oxide Nanoparticles. Chemistry Letters, 2008, 37, 1116-1117.	1.3	10
71	Controlled Synthesis of Monodispersed Cerium Oxide Nanoparticle Sols Applicable to Preparing Ordered Self-Assemblies. Bulletin of the Chemical Society of Japan, 2008, 81, 761-766.	3.2	29
72	Analytical Study of Resistance Drift Phenomena on (PANI) <i>x</i> MoO3 Hybrid Thin Films as Gas Sensors. Bulletin of the Chemical Society of Japan, 2008, 81, 1331-1335.	3.2	9

#	Article	IF	CITATIONS
73	Monitoring of dispensed fluid with the quartz crystal microbalance (QCM) for the better control of inkjet or dispenser machine. Journal of the Ceramic Society of Japan, 2008, 116, 459-461.	1.1	7
74	Development of Hydrogen Sensors and Their Application to Monitoring of Human Condition. Journal of Japan Institute of Electronics Packaging, 2008, 11, 508-512.	0.1	0
75	Thermoelectric Gas Sensor using Au Loaded Titania CO Oxidation Catalyst. Journal of the Ceramic Society of Japan, 2007, 115, 37-41.	1.3	14
76	Highly Aldehyde Gas-Sensing Responsiveness and Selectivity of Layered Organic-Guest/MoO3-Host Hybrid Sensor. Journal of the Ceramic Society of Japan, 2007, 115, 742-744.	1.1	6
77	Preparation of Micro-Thermoelectric Hydrogen Sensor Loading Two Kinds of Catalysts to Enhance Gas Selectivity. Journal of the Ceramic Society of Japan, 2007, 115, 748-750.	1.1	5
78	New Structural Design of Micro-Thermoelectric Sensor for Wide Range Hydrogen Detection. Journal of the Ceramic Society of Japan, 2006, 114, 853-856.	1.3	39
79	Practical Test Methods for Hydrogen Gas Sensor Response Characterization. Electrochemistry, 2006, 74, 315-320.	1.4	8
80	Pt Loaded Alumina Ceramic Catalysts for Micro Thermoelectric Hydrogen Sensors. Journal of the Ceramic Society of Japan, 2006, 114, 686-691.	1.3	1
81	Micro-thermoelectric devices with ceramic combustors. Sensors and Actuators A: Physical, 2006, 130-131, 411-418.	4.1	20
82	Integration of ceramic catalyst on micro-thermoelectric gas sensor. Sensors and Actuators B: Chemical, 2006, 118, 283-291.	7.8	22
83	Catalyst Combustors with B-Doped SiGe/Au Thermopile for Micro-Power-Generation. Japanese Journal of Applied Physics, 2006, 45, L1130-L1132.	1.5	10
84	B- and P-Doped Si _{0.8} Ge _{0.2} Thin Film Deposited by Helicon Sputtering for the Micro-Thermoelectric Gas Sensor. Key Engineering Materials, 2006, 320, 99-102.	0.4	6
85	Micro-Thermoelectric Gas Sensor with P-doped SiGe Thin Film Deposited by Helicon Sputtering. ECS Transactions, 2006, 1, 23-27.	0.5	0
86	Transmission electron microscope observation of the high-pressure form of magnesite retrieved from laser heated diamond anvil cell. Earth and Planetary Science Letters, 2005, 239, 98-105.	4.4	39
87	Mg/Si ratios of aqueous fluids coexisting with forsterite and enstatite based on the phase relations in the Mg ₂ SiO ₄ SiO ₂ H ₂ O system. American Mineralogist, 2004, 89, 1433-1437.	1.9	49
88	Stability of magnesite and its high-pressure form in the lowermost mantle. Nature, 2004, 427, 60-63.	27.8	234
89	High pressure and high temperature phase transitions of FeO. Physics of the Earth and Planetary Interiors, 2004, 146, 273-282.	1.9	51
90	Phase boundary between rutile-type and CaCl ₂ -type germanium dioxide determined by in situ X-ray observations. American Mineralogist, 2002, 87, 99-102.	1.9	28

MAIKO NISHIBORI

#	Article	IF	CITATIONS
91	Post-stishovite phase boundary in SiO2 determined by in situ X-ray observations. Earth and Planetary Science Letters, 2002, 197, 187-192.	4.4	84
92	Construction of laser-heated diamond anvil cell system for in situ x-ray diffraction study at SPring-8. Review of Scientific Instruments, 2001, 72, 1289.	1.3	92
93	Iron partitioning in a pyrolite mantle and the nature of the 410-km seismic discontinuity. Nature, 1998, 392, 702-705.	27.8	137
94	Phase transformations in serpentine and transportation of water into the lower mantle. Geophysical Research Letters, 1998, 25, 203-206.	4.0	90
95	The Postspinel Phase Boundary in Mg2SiO4 Determined by in Situ X-ray Diffraction. Science, 1998, 279, 1698-1700.	12.6	251